HAL
archives-ouvertes.fr

Thin-Film MOSFET-Based Pressure Sensor

Ethan L.W. Gardner, Andrea de Luca, Julien Philippe, Daniela Dragomirescu, Florin Udrea

▶ To cite this version:

Ethan L.W. Gardner, Andrea de Luca, Julien Philippe, Daniela Dragomirescu, Florin Udrea. Thin-Film MOSFET-Based Pressure Sensor. IEEE Sensors Letters, IEEE, 2019, 3 (7), pp.1-4. 10.1109/LSENS.2019.2927694 . hal-02289295

HAL Id: hal-02289295
https://hal.laas.fr/hal-02289295

Submitted on 16 Sep 2019

HAL is a multi-disciplinary open access archive for the deposit and dissemination of scientific research documents, whether they are published or not. The documents may come from teaching and research institutions in France or abroad, or from public or private research centers.

L'archive ouverte pluridisciplinaire **HAL**, est destinée au dépôt et à la diffusion de documents scientifiques de niveau recherche, publiés ou non, émanant des établissements d'enseignement et de recherche français ou étrangers, des laboratoires publics ou privés.

HAL
archives-ouvertes.fr

Thin-Film MOSFET-Based Pressure Sensor

Ethan L.W. Gardner, Andrea de Luca, Julien Philippe, Daniela Dragomirescu, Florin Udrea

▶ To cite this version:

Ethan L.W. Gardner, Andrea de Luca, Julien Philippe, Daniela Dragomirescu, Florin Udrea. Thin-Film MOSFET-Based Pressure Sensor. IEEE Sensors Letters, IEEE, 2019, 3 (7), pp.1-4. 10.1109/LSENS.2019.2927694 . hal-02289295

HAL Id: hal-02289295
https://hal.laas.fr/hal-02289295

Submitted on 16 Sep 2019

HAL is a multi-disciplinary open access archive for the deposit and dissemination of scientific research documents, whether they are published or not. The documents may come from teaching and research institutions in France or abroad, or from public or private research centers.

L'archive ouverte pluridisciplinaire **HAL**, est destinée au dépôt et à la diffusion de documents scientifiques de niveau recherche, publiés ou non, émanant des établissements d'enseignement et de recherche français ou étrangers, des laboratoires publics ou privés.

Thin-Film MOSFET-Based Pressure Sensor

Ethan L.W. Gardner[1,2], Andrea De Luca[1], Julien Philippe[2], Daniela Dromirescu[,2*] and Florin Udrea[1**]
[1]University of Cambridge, Cambridge, United Kingdom
[2]LAAS/CNRS, Toulouse, France
* Senior Member, IEEE
** Fellow, IEEE

Abstract—This paper proposes a silicon-on-insulator (SOI) complementary metal-oxide semiconductor (CMOS) micro-electromechanical system (MEMS) thin-film pressure sensor in which the sensing elements are based on stress sensitive MOSFETs, and the carrier mobility and channel resistance vary with applied pressure. Four MOSFETs are embedded within a silicon dioxide membrane to form a Wheatstone bridge. The sensors are fabricated in a commercial foundry with p-channel and n-channel designs both investigated. The fabricated pMOSFET design gave a pressure sensitivity of 5.21 mV/kPa whilst the nMOSFET gave about half the sensitivity at 2.40 mV/kPa. This was coupled with maximum power consumption of 0.19 mW and 0.39 mW for the pMOSFET and nMOSFET respectively. This shows a highly sensitive pressure sensor, with improved sensitivity on traditional piezoresistors as well as significantly higher sensitivity than current MOSFET based pressure sensors. Moreover, the maximum DC power consumption was only 190 μW and 390 μW for the pMOSFET and nMOSFET, respectively. This novel low-cost, low-power, high-sensitivity CMOS MEMS technology with on-chip electronics could be used towards the implementation of MOSFET based pressure transduction in a multitude of industrial and other applications.

Index Terms—Pressure Sensor, CMOS MEMS, MOSFET, Microfabrication.

I. INTRODUCTION

The most mature industrial use of micromachined sensors revolves around pressure transducers, of which various technologies have been developed including piezoresistive, capacitance, piezoelectric, resonator and others. The inherent nature of micromachining allows these pressure sensors to become small, temporally fast, very accurate and requiring low power consumption. Therefore it is necessary to continue designing and optimizing these technologies that are so industrially desirable for automotive, aerospace, biomedical and many other sectors [1]–[3]. A review on silicon micromachined pressure sensors can be found here [4].

Compared to the well-established piezo-resistor technology [5], [6], there has been little research into using active electronic devices for pressure measurements. However, there has been research into the effect of pressure on transistor channel resistance and carrier mobility [7]–[9], showing the possibility of fabricating pressure sensors where the sensing elements are MOSFETs as opposed to the more traditional piezo-resistors. Previous examples of utilizing active electronic devices in the fabrication of pressure sensors are: a pressure sensor incorporating a stress sensitive MOS operational amplifier [10]; a pressure sensor using two embedded MOSFETs and two embedded resistors in the Wheatstone bridge configuration [11]; the fabrication and modelling of a pressure sensitive FET [12]; the use of a polyimide sacrificial layer and suspension gate MOSFET [13]; a nc-Si/c-Si heterojunction MOSFET pressure sensor [14] showing a sensitivity of 2.15 mV/kPa and the design of a mirror sensing based MOSFET embedded pressure sensor [15]. Finally, [16] uses the piezo-MOS effect within a pressure sensitive differential amplifier. A collation of the technologies and their sensitivities can be found in Table 1 alongside the technology illustrated in the paper.

Table 1. Table showing current technologies and their sensitivities.

Reference	Sensitivity (mV/kPa)	Sensing Element
[5]	1.14	Piezo-resistor
[6]	0.051	Piezo-resistor
[11]	0.125	Piezo-resistor + MOSFET
[14]	2.153	nc-Si/c-Si heterojunction MOSFET
[15]	0.473	MOSFET Current Mirro Circuit
[16]	1.29	MOSFET Differential Amplifer
pMOS	5.21	pMOSFET
nMOS	2.40	nMOSFET

In this paper, a novel pressure sensor is designed using a standard 1.0 μm SOI CMOS fabrication process and embedding four MOSFETs as the pressure sensitive transduction elements. Both the nMOSFET and pMOSFET design are characterized to effectively

[C]orresponding author: F. A. Author (f.author@psu.edu). If some authors contributed equally, write here, “F. A. Author and S. B. Author contributed equally.” IEEE Sensors Letters discourages courtesy authorship; please use the Acknowledgment section to thank your colleagues for routine contributions.
Digital Object Identifier: 10.1109/LSEN.XXXX.XXXXXXX (inserted by IEEE).

compare them to each other and existing similar technology, striving for low-power high sensitivity sensing solutions. The proposed technology offers suitable characteristics for advancing this area including high sensitivity and low power consumption.

II. DESIGN AND FABRICATION

The piezo-MOSFET sensors investigated in the report were designed using the software Cadence Virtuoso Layout Editor (IC 5.1.4). A 1.0 µm SOI CMOS fabrication process with tungsten metallization was utilized through a commercial foundry. In order to create the thin membrane structure, Deep Reactive Ion Etching (DRIE) was used to etch the back-side silicon, leaving a membrane of approximately 4.5 µm remaining. A picture illustrating the top of the fabricated sensor is shown in Figure 1. Figure 2 shows a detailed view of the layer fabrication and where the sensing elements are located within the membrane, as well as a detailed view of the MOSFET design. Located within the single crystal silicon layer are the 4 piezo-MOSFETS connected to pads *via* 4 µm tracks for source and drain and a 9 µm track for the gate. Two types of MOSFET were designed and tested including pMOSFET and nMOSFET with identical geometric sizes for all the incorporated regions. The p-type design used a crystallographic orientation in the [110] plane whilst the n-type design used the [100], as these have been shown to be the optimum orientation [17].

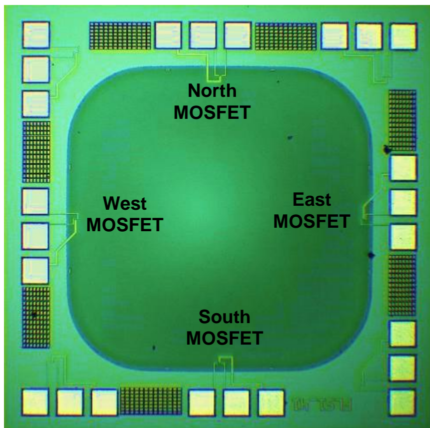

Figure 1. Optical micrograph of the fabricated sensor with MOSFET location illustrated.

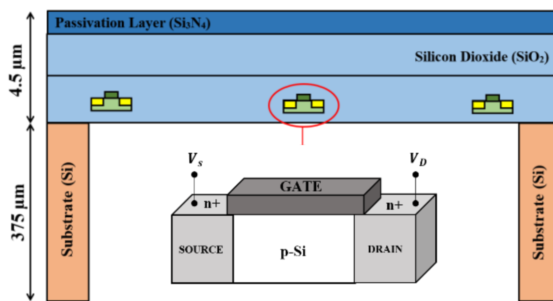

Figure 2. Cross-section of the sensor showing the layer technology and the design of the MOSFETs.

III. EXPERIMENT

The sensor requires a pressure difference between the top and bottom (within the cavity) of the membrane, thus requiring hermetic sealing that ensures no leakage over time for absolute pressure measurements. Using a cleaned glass substrate, a square of thermal epoxy resin (EPO-TEK H20E) was applied using a high precision dispensing machine (Tresky 3000). The sensors were pressed onto the epoxy gel, followed by dispensing the gel along every edge of the sensor to fill in any gaps. The substrate and sensors were then cured in an over for 45 minutes at 120 °C, allowing the resin to become hard.

A SUSS MicroTec PMC200 Cryogenic Probe Station was used to create a pressure difference. Three internal DC probes were connected from the sensor pads to two external Keithley 2450's in order to bias and measure the MOSFETs, all which were controlled by an in-house developed Labview program. The source-drain voltage was swept from 0 to ±5 V in increments of 0.25 V for each gate voltage from 0 to ± 5 V in steps of 1 V. This was carried out for all 4 MOSFETs located on the membrane. This electrical characterization was subsequently repeated at seven pressure differences from 0 to minus 700 mBar (where 0 mBar is atmospheric pressure), whilst maintaining a consistent temperature of 25 °C. In addition to these, measurements were taken over a period of 24 hours at -500 mBar and showed that the hermetic sealing worked as there was no significant leakage during this time period.

The MOSFETs exploit the piezoresistive effect induced by the sensitivity of carrier mobility under applied stress. The drain current of a device operated in the saturation region is given by

(1)

where μ represents the carrier mobility through the channel, is the capacitance of the oxide per unit area, and L are the width and length of the channel, respectively, is the gate voltage and is the threshold voltage. Due to the MOSFET being operated in the saturation region, the channel resistance, R, is equal to the output resistance of the MOSFET which can be calculated through

(2)

Due to the geometric designs in this report remaining the same, W, and can be assumed constant. The normalized change in drain current can then be written as

(3)

It is shown by [7] that the variation in drain current from applied mechanical stress is solely due to the change in carrier mobility μ) and therefore the second term in equation 3 can be neglected. With the addition of a Wheatstone bridge and an applied pressure difference, the voltage output V_{out} changes due to the changing

channel resistances of the Wheatstone bridge arms. This is because the MOSFETs in different arms will change in the opposite direction due to the resistors longitudinally or transversely stressed, thus greatly benefitting from a Wheatstone bridge configuration. The voltage output can be calculated through the following equation

(4)

where R is the channel resistance of the MOSFET with its location on the membrane denoted by the subscript and V_{Wb} is the supplied constant bridge voltage. V_{out} is subsequently used to investigate and characterize the sensor response and performance with pressure. Knowing that $\Delta R_{Out} = \Delta V_{DD}/\Delta I_{DS}$, we can substitute equations 2 and 3 into the Wheatstone bridge equation (eq. 4) and show how the change in voltage output depends on the carrier mobility. This can be further simplified assuming the MOSFETs display identical behavior and that the two arms of the Wheatstone bridge will behave equally and opposite where the subscripts 1 and 2 refer to the opposite arms of the Wheatstone bridge.

(5)

The circuit schematic of the pressure sensor is shown in Figure 3 where (a) shows the Wheatstone bridge configuration comprising of the four pressure sensitive MOSFETs, and (b) shows the equivalent circuit when their channel resistances are taken as the piezo resistances.

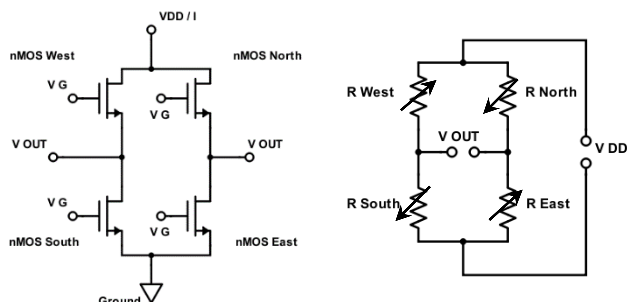

Figure 3. Schematic showing the operation of the MOSFET pressure sensor for (a) Wheatstone bridge operation and (b) the equivalent circuit as piezo resistances. *N.B.* V_G was held constant for all 4 MOSFETs.

IV. RESULTS AND DISCUSSION

A. MOSFET Characteristics

Initially, it is important to look at the behavior of the MOSFET when the pressure remains constant. Figure 4 shows the characteristic curves for the on-membrane pMOSFET (left) and nMOSFET (right) at atmospheric pressure, which is the current from drain to source I_{DS} plotted against the voltage from drain to source for varying gate voltage V_G. This figure shows the conventional functioning of MOSFETs with clear linear and saturation regions for both designs. This proves the designs function properly and were not corrupted during the design or fabrication phases. This also provides the information in order to bias the devices in the saturation region. As expected, the drain current of the nMOSFET is approximately twice as large as the pMOSFET, which is due to carrier mobility being 2.5 times higher for electron mobility as opposed to hole mobility.

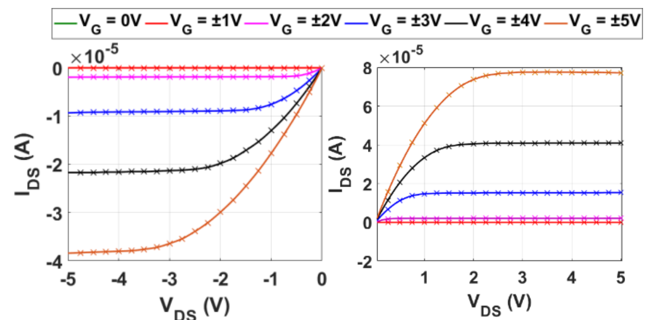

Figure 4. The characteristic curves of the pMOSFET (left) and the nMOSFET (right). V_G is negative for the p-device and positive for the n-device.

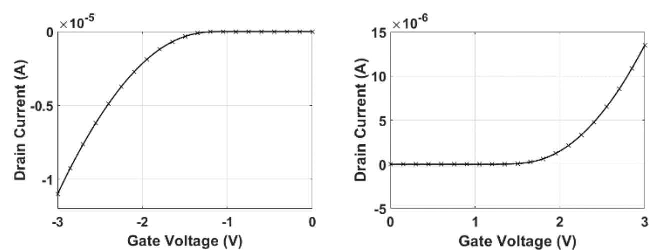

Figure 5. The drain current against gate voltage for pMOSFET (left) and nMOSFET (right) for calculating the threshold voltage.

Figure 5 shows the drain current plotted against the gate voltage, commonly known as the threshold curve. The threshold voltage V_T was calculated by plotting the square root if the drain current and taking the gate voltage intercept from the linear region of the curve. The pMOSFET design has a threshold voltage of -1.2 V whilst the nMOSFET displayed a threshold voltage of +1.5 V. The knowledge of these threshold voltages provides the point at which the devices turn on, and thus allowing the region of biasing to be used when measuring the response to pressure.

B. Response to Pressure

The experimental stage provided the full characteristic curves of all 4 membrane MOSFETs at every pressure difference. These were then converted into channel resistances and equation 2 was used to attain a voltage output of the sensors with the increasing of pressure difference, which is illustrated in Figure 6. Figure 6 (a) and (b) show the voltage response whilst varying the drain voltage and keeping the gate voltage at ±5 V. Figure 6 (c) and (d) show the

voltage response for varying gate voltage and constant drain voltage. It can be seen that varying the drain current has no effect on the voltage response, meaning that the lowest drain voltage possible should be used for the lowest power consumption. For all gate voltages above the threshold voltage, there is a strong increase in output voltage with increasing pressure. It can be seen that for the gate voltages of ±2 V, the response is slightly higher, which can be ascribed to their functioning being within the ohmic region. Most importantly, the full-scale output voltage of the pMOSFET (0.21 V) is much larger than for the nMOSFET (0.096).

Using the data displayed in Figure 6, important performance parameters can be evaluated. Firstly, the voltage sensitivity, S, is calculated through

(3)

where P_m and P_i are the maximum and considered pressures respectively and $V_{Out}(P_m)$ and $V_{Out}(P_i)$ denote their voltage output. The maximum sensitivity of the pMOSFET design is 5.21 mV/kPa whilst the nMOSFET design came out with a lower sensitivity of 2.40 mV/kPa. The total consumed power can also be calculated using $Power = V_{DS} \cdot I_{DS}$, resulting in a maximum power consumption of 0.19 mW for the pMOSFET and 0.39 mW for the nMOSFET. These
performance parameters demonstrate a highly sensitive, low-power MEMS pressure transducer.

These results can be compared with existing technologies that use pressure sensitive MOSFETs using Table 1. Here it can be seen that the device presented in this report improves on the highest recorded sensitivity documented by 240%, even before any geometrical optimization. The device shows a large increase on other MOSFET-based designs and is also more sensitive than many recent piezo-resistive sensors whilst requiring a lower power consumption.

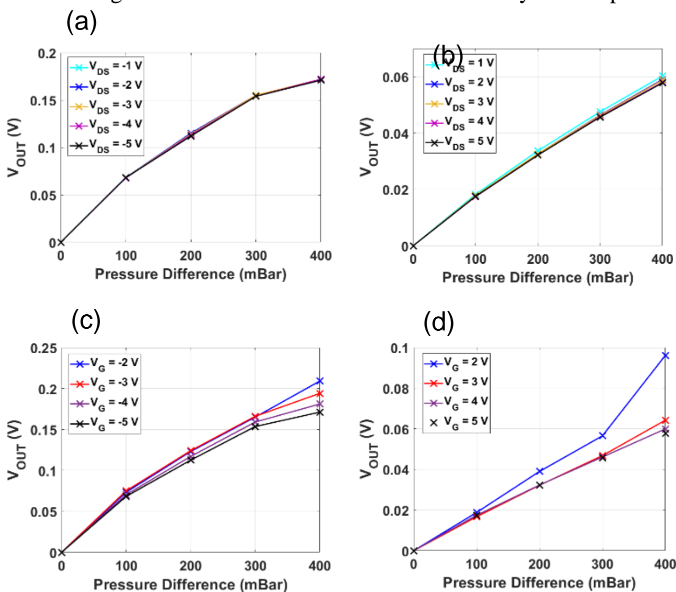

Figure 6. The change in voltage output with the evolution of pressure for (a) pMOSFET with varying drain voltage, (b) nMOSFET with varying drain voltage, (c) pMOSFET with varying gate voltage and (d) nMOSFET with varying gate voltage.

V. CONCLUSION

The design, fabrication, experiment and results of a novel MOSFET-based pressure sensor are reported. The design embeds 4 MOSFETs within a thin silicon dioxide membrane *via* CMOS MEMS technology and incorporates a Wheatstone bridge in order to relate the change in carrier mobility through the MOSFET channel to the change in pressure. The pMOSFET shows the highest sensitivity of 5.21 mV/kPa, showing significant improvement on other MOSFET-based technologies in addition to piezo-resistive designs whilst retaining a low power consumption. This shows great promise for the future of MOSFET pressure sensors.

ACKNOWLEDGMENT

This research was partly funded through the Eiffel Scholarship scheme, providing a collaboration between the University of Cambridge and LAAS/CNRS.

REFERENCES

[1] W. J. Fleming, 'Overview of automotive sensors', *IEEE Sens. J.*, vol. 1, no. 4, pp. 296–308, 2001.
[2] S. Samaun, K. Wise, E. Nielsen, and J. Angell, 'An IC piezoresistive pressure sensor for biomedical instrumentation', in *1971 IEEE International Solid-State Circuits Conference. Digest of Technical Papers*, 1971, vol. 14, pp. 104–105.
[3] R. S. Okojie, J. C. DeLaat, and J. R. Saus, 'SiC pressure sensor for detection of combustor thermoacoustic instabilities [aircraft engine applications]', in *The 13th International Conference on Solid-State Sensors, Actuators and Microsystems, 2005. Digest of Technical Papers. TRANSDUCERS'05.*, 2005, vol. 1, pp. 470–473.
[4] K. N. Bhat, 'Silicon micromachined pressure sensors', *J. Indian Inst. Sci.*, vol. 87, no. 1, p. 115, 2012.
[5] S. Chen, M. Zhu, B. Ma, and W. Yuan, 'Design and optimization of a micro piezoresistive pressure sensor', in *2008 3rd IEEE International Conference on Nano/Micro Engineered and Molecular Systems*, 2008, pp. 351–356.
[6] V. Sandrimani and K. B. Balavalad, 'Design and Simulation of Silicon on Insulator Based Piezoresistive Pressure Sensor', p. 7, 2018.
[7] A. T. Bradley, R. C. Jaeger, J. C. Suhling, and K. J. O'Connor, 'Piezoresistive characteristics of short-channel MOSFETs on (100) silicon', *IEEE Trans. Electron Devices*, vol. 48, no. 9, pp. 2009–2015, 2001.
[8] R. Vatedka, H. Takao, K. Sawada, and M. Ishida, 'Effect of high drain voltage on stress sensitivity in nMOSFETs', *Sens. Actuators Phys.*, vol. 140, no. 1, pp. 89–93, 2007.
[9] J.-M. Sallese, W. Grabinski, V. Meyer, C. Bassin, and P. Fazan, 'Electrical modeling of a pressure sensor MOSFET', *Sens. Actuators Phys.*, vol. 94, no. 1–2, pp. 53–58, 2001.
[10] L. Jingjing, Y. Ruifeng, and L. Litian, 'MOSFET differential amplifier with input pair and active load pair being stress-sensitive both', in *2001 6th International Conference on Solid-State and Integrated Circuit Technology. Proceedings (Cat. No. 01EX443)*, 2001, vol. 2, pp. 812–815.
[11] Z.-H. Zhang, Y.-H. Zhang, L.-T. Liu, and T.-L. Ren, 'A novel MEMS pressure sensor with MOSFET on chip', in *SENSORS, 2008 IEEE*, 2008, pp. 1564–1567.
[12] R. S. Jachowicz and Z. M. Ażgin, 'FET pressure sensor and iterative method for modelling of the device', *Sens. Actuators Phys.*, vol. 97, pp. 369–378, 2002.
[13] M. Fernández-Bolaños *et al.*, 'Polyimide sacrificial layer for SOI SG-MOSFET pressure sensor', *Microelectron. Eng.*, vol. 83, no. 4–9, pp. 1185–1188, 2006.
[14] X. Zhao, D. Wen, and G. Li, 'Fabrication and characteristics of an nc-Si/c-Si heterojunction MOSFETs pressure sensor', *Sensors*, vol. 12, no. 5, pp. 6369–6379, 2012.
[15] P. K. Rathore and B. S. Panwar, 'Design and optimization of a CMOS-MEMS integrated current mirror sensing based MOSFET embedded pressure sensor', in *2013 IEEE International Conference on Control Applications (CCA)*, 2013, pp. 443–448.
[16] V. Garcia and F. Fruett, 'A mechanical-stress sensitive differential amplifier', *Sens. Actuators Phys.*, vol. 132, no. 1, pp. 8–13, 2006.
[17] Y. Kanda, 'A graphical representation of the piezoresistance coefficients in silicon', *IEEE Trans. Electron Devices*, vol. 29, no. 1, pp. 64–70, 1982.